Effects of saturating metabolic uptake on space profiles and tracer kinetics

CARL A. GORESKY, GLEN G. BACH, AND COLIN P. ROSE
McGill University Medical Clinic, Montreal General Hospital and Departments of Medicine, Physiology, and Mechanical Engineering, McGill University, Montreal, Quebec HG3 1A4, Canada

GORESKY, CARL A., GLEN G. BACH, AND COLIN P. ROSE. *Effects of saturating metabolic uptake on space profiles and tracer kinetics.* Am. J. Physiol. 244 (Gastrointest. Liver Physiol. 7): G215-G232, 1983.—Vascular and steady-state lengthwise concentrations evolving in tissue as a consequence of saturable uptake processes are explored when there is no effective barrier between blood and tissue, when there is one effective barrier (the liver), and when barriers are present at both capillary and cell membrane. Falling exponential profiles develop at low-input concentrations and grade over into much smaller linear decreases at high concentrations. Uptake behind an effective barrier produces a step-down in concentration. With no effective barriers, a tracer impulse propagates to the outflow in a delayed fashion, reversible binding to the enzymic removal mechanism increasing its space of distribution and delaying it further and irreversible uptake diminishing its area. As bulk concentration is increased, proportional tracer uptake diminishes and ultimately approaches zero. With barriers in the system, tracer output consists of an impulse damped by cell entry, followed by outflow recovery of material that has escaped cell uptake. Increase in bulk concentration is found to saturate the uptake mechanism, with a proportionate increase in the returning material.

steady-state space concentration profiles; Michaelis-Menten kinetics; nonlinear kinetics; tracer uptake studies; saturation effects on tracer outflow profiles; hepatic uptake processes; capillary and tissue concentration profiles; space effects at tracer concentration

TRACER KINETICS have now long been used to study the handling and disposal of substances in the circulation. Gross descriptions of the manner in which the liver, for instance, removes material from the circulation have been derived, and in the steady state linearized tracer kinetics have been used to derive parameters corresponding to cellular exchange rates and intracellular disposal rates (10, 11, 14). Metabolic disposal processes are characteristically nonlinear [the cellular metabolic disposal of galactose, for instance, exhibits saturation kinetics when it is explored over a wide range of plasma concentrations (11, 26), and the secretion in bile of those organic anions excreted at a high concentration shows a characteristic transport maximum (27)]. Linearization of the saturating kinetic processes provides an approach to the problem, but this approximation is valid, in each instance, over only a small concentration range. The more general problem of dealing with the nonlinearity remains.

In the present work we deal particularly with events at the level of a single vascular channel. We analyze the relation between steady-state and tracer kinetics in the saturating case and compare the results with the linear case. The effects of the presence and absence of effective barriers between the blood and cellular contents are explored. Analytical descriptions are pursued particularly because of the insight into the problem that they provide. The simpler and then the more complex problems are explored.

Underlying Steady State When There Are No Effective Barriers in System

Derivation of equations describing behavior of substrate. Suppose that a substance is being carried through a liver sinusoid by flow with velocity, W; that within the sinusoid it freely permeates red cells, the space of Disse, and the parenchymal cells in a nonconcentrative fashion; and that the space accessible to the substance at each of these sites is β, γ, and θ times that present in sinusoidal plasma. Further assume that there is bolus flow in the system (red cells and sinusoidal plasma are then carried along at the same rate) and that there is a metabolic disposal process distributed uniformly along the sinusoid from input at $x = 0$ to exit at $x = L$, described by Michaelis-Menten kinetics, with V_{max} equaling the maximal removal rate per volume of cells and K_m equaling the concentration at which half-maximal removal occurs. With the dimensions of a sinusoid and its associated half-cell sheet, diffusion equilibration will occur laterally at each point along the length, but transport along the length, the larger dimension of the system, will occur only by flow (2, 3, 8).

In deriving the equation to describe the behavior of substrate in this system, some detail of the mechanism is also needed. In the accompanying paper Goresky et al. (13) showed, at the experimental level, that the reversible association of some tracer alcohols with the intracellular enzyme mediating their conversion to product is visible from the plasma phase as a space of distribution for tracer inside the liver cells, larger than that accessible to tracer water. The effect is especially large when no bulk alcohol is present. We must account both for these new observations and for classical saturation effects (4, 17, 21). The key to both lies in enzyme kinetics. Consider first that, in the steady state, substrate u combines with the enzyme e to form an enzyme-substrate complex eu with the rate constant k_a. The complex either dissociates

0193-1857/83/0000-0000$01.50

to form e and u with the rate constant k_d or proceeds to form the product p with the rate constant k_s, viz

$$e + u \underset{k_d}{\overset{k_a}{\rightleftarrows}} eu \xrightarrow{k_s} e + p \tag{1}$$

Now if we define the Michaelis constant of the reaction

$$K_m = \frac{k_d + k_s}{k_a} = \frac{[e][u]}{[eu]} \tag{2}$$

and the total enzyme concentration as

$$[e_T] = [e] + [eu] \tag{3}$$

we find

$$\frac{[eu]}{[u]} = \frac{[e_T]}{[u] + K_m} \tag{4}$$

Substrate will be present within the cells in both bound and free forms in the ratio described by the above relation. From the point of view of the plasma, at any point along the sinusoidal length or at the outflow, substrate will appear to have entered both the free substrate pool within the cellular space and the additional bound substrate pool, whose incremental size is described by the ratio $[eu]/[u]$.

At the experimental level, the behavior of this ratio both at the asymptotic concentration extremes and in the presence of inhibitor is of interest.

a) When $[u] \to 0$

$$\frac{[eu]}{[u]} \to \frac{[e_T]}{K_m} \tag{5a}$$

Substrate, in vanishingly low concentrations, will see an incremental space that reflects the concentration of enzymic binding sites and that varies inversely with the K_m (the additional space effect thus becomes large when K_m is small).

b) When $[u]$ becomes large

$$\frac{[eu]}{[u]} \to 0 \tag{5b}$$

At high substrate concentrations the incremental space virtually disappears.

c) Finally, when an inhibitor $[i]$ is present in the system that also binds to the enzyme, the ratio describing the incremental space accessible to tracer becomes

$$\frac{[eu]}{[u]} = \frac{[e_T]}{[u] + K_m(1 + [i]/K_i)} \tag{5c}$$

where $K_i = [e][i]/[ei]$. By its presence, the inhibitor reduces the size of the incremental space accessible to substrate.

The rate of substrate removal is also nonlinear. The bulk substrate removal rate V is found by

$$V = k_s[eu] \tag{6a}$$

$$= \frac{k_s[e_T][u]}{[u] + K_m} \tag{6b}$$

where $k_s[e_T] = V_{max}$, the maximal removal rate in the system.

With this background, the partial differential equation describing concentration within the system as a function of space and time can be formulated as follows: change in local substrate = −change due to axial convection in blood − change due to cellular removal or

$$(1 + \beta + \gamma + \theta[1 + e_T/\{u + K_m\}])\frac{\partial u}{\partial t} = -(1 + \beta)W\frac{\partial u}{\partial x} - V_{max}\theta\frac{u}{u + K_m} \tag{7a}$$

from which

$$\frac{(1 + \beta + \gamma + \theta[1 + e_T/\{u + K_m\}])}{(1 + \beta)W}\frac{\partial u}{\partial t} + \frac{\partial u}{\partial x} + \frac{V_{max}\theta u}{(1 + \beta)W(u + K_m)} = 0 \tag{7b}$$

where $u(x, t)$ is the concentration of substrate in the system at the place x along the length and at the time t.

Steady-state concentration profiles. Now examine the steady-state concentration profiles at long time, when the input concentration has been set at u_o. The change in concentration is then a function of x only and is described by the ordinary differential equation

$$\frac{du}{dx} + B\frac{u}{u + K_m} = 0 \tag{8}$$

where $B = V_{max}\theta/(1 + \beta)W$. From this

$$\left(\frac{u + K_m}{u}\right)du = -B dx \tag{8a}$$

$$u^{K_m}e^u = u_o^{K_m}e^{u_o}e^{-Bx} \tag{9}$$

or

$$\left(\frac{u}{u_o}\right)^{K_m} e^{u-u_o} = e^{-\frac{V_{max}\theta}{1+\beta}\frac{x}{W}} \tag{9a}$$

or

$$K_m(\ln u_o - \ln u) + u_o - u = \frac{V_{max}\theta}{1 + \beta}\frac{x}{W} \tag{9b}$$

The concentration u is an implicit function of distance in the steady state. Values for $u(x)$ cannot be found directly but can be conveniently calculated numerically by forming a function of the difference between the two sides of *Eq. 9a* and then optimizing initial estimates of u by the secant method (22) until this function is zero for given values of x/W and the other parameters.

The asymptotic extremes are of particular interest.

a) If u_o and $u \ll K_m$, then $(u_o + K_m) \to K_m$ and $(u + K_m) \to K_m$. In this extreme, *Eq. 8* becomes

$$\frac{du}{dx} + \frac{B}{K_m}u = 0 \tag{10}$$

from which

$$u = u_o e^{-\frac{V_{max}\theta}{(1+\beta)K_m}\frac{x}{W}} \tag{11}$$

At low concentrations the concentration decreases exponentially along the length.

The exponential decrease is the kind expected in the linear case, in which removal takes place in proportion to the concentration (as in *Eq. 10*). There is a V_{max}/K_m dependence in the removal rate constant.

b) If u_o and $u \gg K_m$, then $(u_o + K_m) \rightarrow u_o$ and $(u + K_m) \rightarrow u$. In this extreme, *Eq. 8* becomes

$$\frac{du}{dx} + B = 0 \qquad (12)$$

where

$$du = -\frac{V_{max}\theta}{1+\beta}\frac{x}{W} \qquad (12a)$$

from which

$$u = u_o - \frac{V_{max}\theta}{1+\beta}\frac{x}{W} \qquad (13)$$

In this extreme the steady-state concentration profile decreases linearly along the length. The amount of material removed per unit time in the completely saturated system becomes maximal (it is independent of the concentration), and the rate of lengthwise decline in concentration varies inversely with the velocity of flow, W. At constant W, it is dependent only on V_{max}.

Goresky (8) has shown experimentally that labeled water is distributed into the space of Disse and the parenchymal cells in a flow-limited manner and that the red cell membrane is not limiting to its exchange (12). Goresky et al. (13) have shown that tracer ethanol is distributed into the liver in a manner indistinguishable from labeled water when its uptake has been saturated by intravenous infusion of ethanol. In Figs. 1 and 2, we have utilized the characteristic parameters arising from that study in order to portray the expected steady-state ethanol concentration profiles along liver sinusoids with mean transit (τ) values of 2 and 10 s for a variety of input concentrations. In each case a single profile is presented because the concentration in cells adjacent to the sinusoid will be expected to be the same as that in the sinusoid. The progressive change in shape of the lengthwise profile from a proportionately major exponential decline at low plasma concentrations to a small-scale linear decrease at high concentrations is illustrated.

Use of experimental input and output concentrations. Bass et al. (1) and Keiding et al. (20) have examined uptake in a system in which they hypothesized the uptake mechanism to be situated at the wall of the sinusoid (this is analogous to the alcohol uptake case, except that the volume of the cells is not explicitly considered in developing the equations). In this instance, they found a way to avoid consideration of the implicit solution presented above. Their approach is characterized by the incorporation of an experimentally observable quantity, the net rate of removal, ν, across the sinusoid-hepatocyte unit, where, if u_L is the outflow sinusoidal concentration at $x = L$ and F_w is the flow of blood water in the system, $\nu = F_w(u_o - u_L)$.

Now reexamine the steady-state equation (*Eq. 8*)

$$\frac{du}{dx} = -\frac{\theta}{(1+\beta)W} V_{max}\frac{u}{u+K_m}$$

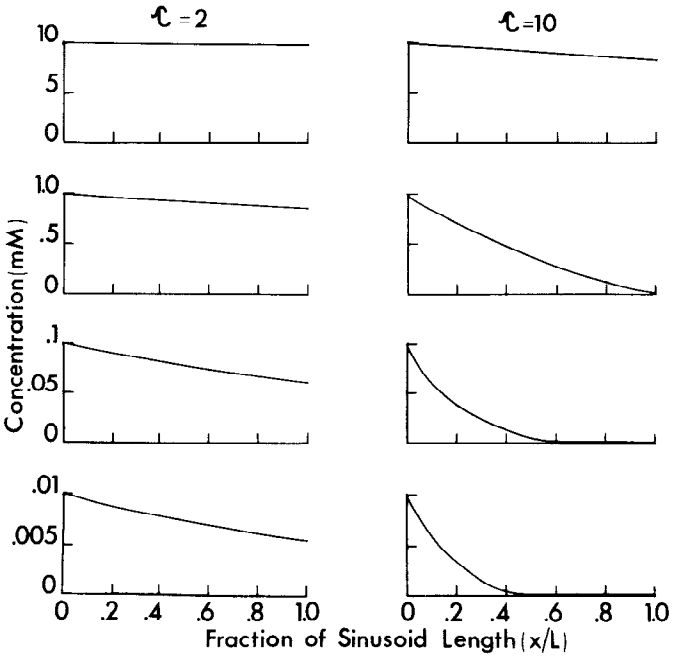

FIG. 1. Steady-state ethanol concentrations displayed as a function of sinusoidal length. Input ethanol concentrations are those recorded at $x/L = 0$. *Left-hand panels*: mean transit time(τ) of 2 s; *right-hand panels*: mean transit time of 10 s. Characteristic parameters utilized for calculations were those obtained by Goresky et al. (13): a K_m value of 0.33 mM, a V_{tot} value of 0.0247 mmol·s^{-1}·(l liver water)$^{-1}$, and V_{max} value of 0.0352 mmol·s^{-1}·(l liver cell water)$^{-1}$.

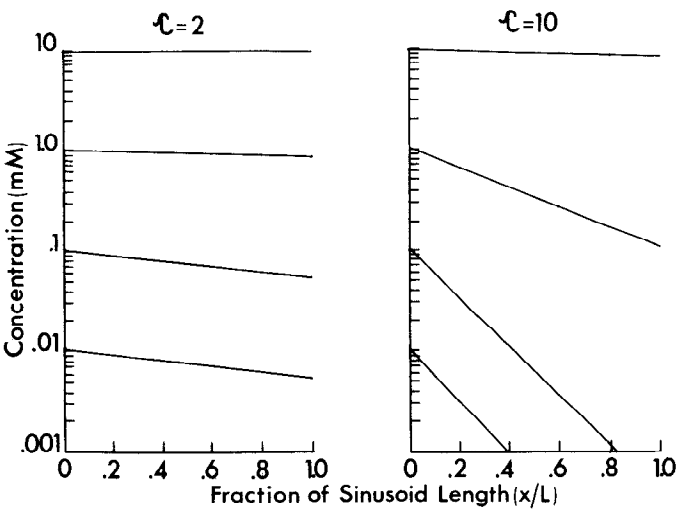

FIG. 2. Data from Fig. 1 plotted against a continuous logarithmic concentration scale. Relative alteration in concentration-space profiles, with change in input concentration and change in sinusoidal mean transit time, becomes apparent with this kind of display.

and disarticulate the ratio $\theta/(1 + \beta)$. It is equal to the ratio of C/Bl_w, where C is the cellular water space per unit length and Bl_w is the sinusoidal blood water space per unit length [the product of $(1 + \beta)$ and the sinusoidal plasma water content per unit length]. Then, because $F_w = Bl_w W$

$$F_w\left(1 + \frac{K_m}{u}\right) du = -V_{max} C dx \qquad (14)$$

The definite integral of Cdx from $x = 0$ to $x = L$ will be

equal to the total volume of the cells in a sinusoidal unit. If the product of this and V_{max} is V_{tc} we find, after integrating the equation and substituting for F_w, the expression

$$\nu + \nu K_m \frac{(\ln u_o - \ln u_L)}{(u_o - u_L)} = V_{tc}$$

If $\hat{u}$ is defined by the expression

$$\hat{u} = \frac{u_o - u_L}{\ln u_o - \ln u_L}$$

then

$$\nu = \frac{V_{tc}\hat{u}}{\hat{u} + K_m} \qquad (15)$$

The values for ν, the product of flow and the concentration difference across the sinusoid, and the values for $\hat{u}$, based on these concentration differences, could be determined for a range of concentrations if sinusoidal inflow and outflow concentrations were accessible; from these, values for V_{tc} and K_m could be obtained.

The whole organ. The expressions outlined above are those for a single hepatic sinusoid. In the whole liver there are many acini and, within each acinus, many sinusoids perfused in parallel. One might assume that, within the whole organ, there might be an unchanging distribution of transit time or x/W values and that, with this, V_{max} (or enzyme content) might be induced in such a fashion that it is largest where delivery is largest along large-flow channels. However, direct visual observations (23) indicate that there is an inherent random rhythmicity in the microcirculatory flow patterns of the organ, groups of sinusoids asynchronously shifting their flows in such a manner that although each area varies there is a stability to the pattern as a whole. No constant linkage between V_{max} and x/W is then possible. The heterogeneity in flows or transit times will be expected to be dominant, and with a common inflow concentration there will be a corresponding distribution of sinusoidal outflow concentrations. Observed mixed venous outflow concentrations will necessarily represent flow-weighted mean values for the whole assembly.

This presents a problem in terms of relating the single-sinusoid expression to events at the level of the whole liver. When only steady-state inflow and mixed outflow concentrations are available, the transit time heterogeneity, with its influence on various sinusoid outflow concentrations, is not accessible. Keiding et al. (19), for instance, have applied the expression for the single sinusoid to a set of inflow and mixed venous outflow values, neglecting any heterogeneity, and have calculated characteristic parameters for the ethanol disposal system. On the basis of past studies of heterogeneity (Refs. 7 and 24 and J. B. Bassingthwaighte and C. A. Goresky, unpublished observations), one would expect the maximal enzymic disposal rate to have been underestimated when the single-sinusoidal model is utilized. It was the aim of our accompanying experimental study (13) to determine whether the multiple-indicator dilution approach could provide additional information (it led to the experimental discovery of the enzyme incremental space effect) and to develop a way of estimating the characteristic parameters of the enzymatic disposal system from tracer data while taking into account the heterogeneity of the sinusoidal transit times.

Pulse-load experiments. In this system, in which there are no barriers, a step input results immediately (after a suitable transport lag) in its corresponding steady-state output concentration. The response of the system to a pulse-type load is then also predictable. Because the system is nonlinear the Dirac delta function formalism cannot be used. Instead, the pulse must be treated as a step-up of a certain finite duration that is succeeded by a step-down. The concentration in the bolus becomes the important factor; the output concentration is automatically fixed for a given pulse-input concentration and transit time. The inference of the foregoing is that the way a pulse load is administered will be of importance in determining the outflow response, inasmuch as the concentration in the pulse will depend on the amount of material injected and the duration of the injection. Experimental procedures can be standardized in such a way that a concordant data set can be defined that illustrates a saturation phenomenon (9), but the general problem remains and cannot be resolved: knowing the concentration within the bolus input. The use of this kind of input must therefore ordinarily be construed to be bad experimental design.

Tracer Studies in a Steady State When There Are No Effective Barriers in System

In the system just described, suppose that a tracer experiment is carried out at a time when the system is in steady state as to bulk concentration, that the tracer is taken up by the enzymic disposal mechanism, and that the products are either sequestered (so they do not return to the system) or are recognizably different from the parent tracer. To reconstruct events within the steady lengthwise concentration profile for substrate, we must distinguish unlabeled and tracer molecules. Let the steady-state concentration at any point be $u = u' + u^*$, where u' represents the unlabeled species and u^* is the labeled species.

Substituting into *Eq. 7b* we find

$$\frac{(1 + \beta + \gamma + \theta[1 + e_T/\{u + K_m\}])}{(1 + \beta)W}\frac{\partial(u' + u^*)}{\partial t} + \frac{\partial(u' + u^*)}{\partial x} + \frac{V_{max}\theta}{(1 + \beta)W}\left(\frac{u' + u^*}{u' + u^* + K_m}\right) = 0 \qquad (16)$$

Now let us examine the expression $(u' + u^*)/(u' + u^* + K_m)$ in the right-hand term. The flux of material being converted by the enzyme will be proportional to this. It will consist of two parts: *1)* $u^*/(u' + u^*)$ times the expression, corresponding to the flux of labeled molecules; and *2)* $u'/(u' + u^*)$ times the expression, corresponding to the flux of unlabeled material. The first part equals

$$\left[\frac{(u'+u^*)}{(u'+u^*+K_m)}\right]\left[\frac{u^*}{(u'+u^*)}\right]$$

$$=\frac{u^*}{u'+u^*+K_m}$$

$$=\frac{u^*}{(u'+K_m)(1+u^*/[u'+K_m])}$$

$$=\frac{u^*}{u'+K_m}-O(u^*)^2+\ldots$$

to a first-order approximation. The converse fraction, which corresponds to flux of unlabeled material through the enzymic conversion mechanism, is

$$\left[\frac{(u'+u^*)}{(u'+u^*+K_m)}\right]\left[\frac{u'}{(u'+u^*)}\right]$$

$$=\frac{u'}{u'+u^*+K_m}=\frac{u'}{u+K_m}$$

At the same time the steady-state condition indicates that

$$\frac{\partial u}{\partial t}=\frac{\partial u'}{\partial t}+\frac{\partial u^*}{\partial t}=0 \tag{16a}$$

Yet, conservation considerations also indicate that if we use the two terms resolved above

$$\frac{(1+\beta+\gamma+\theta[1+e_T/\{u+K_m\}])}{(1+\beta)W}\frac{\partial u'}{\partial t}+\frac{\partial u'}{\partial x}+\frac{V_{max}\theta}{(1+\beta)W}\left(\frac{u'}{u+K_m}\right)=0 \tag{16b}$$

and

$$\frac{(1+\beta+\gamma+\theta[1+e_T/\{u+K_m\}])}{(1+\beta)W}\frac{\partial u^*}{\partial t}+\frac{\partial u^*}{\partial x}+\frac{V_{max}\theta}{(1+\beta)W}\left(\frac{u^*}{u'+K_m}\right)=0 \tag{16c}$$

The radiochemical concentrations of u^* justify the use of the first-order approximation for the third term in *Eq. 16c*, and the tracer condition $u^* \lll u'$ means that $u' \rightarrow u$. The equation that we need to solve in order to describe tracer behavior is *Eq. 16c*, with u' in the denominator of the right-hand term equal to u. At the same time the steady-state condition (*Eq. 8*) is

$$\frac{\partial u}{\partial x}+\frac{V_{max}\theta}{(1+\beta)}\frac{x}{W}\left(\frac{u}{u+K_m}\right)=0$$

still holds; so in *Eq. 16b*, for unlabeled material, $\partial u'/\partial t$ (which equals $-\partial u^*/\partial t$) is very small in relation to $\partial u'/\partial x$.

Equation 16c presents a linkage between u^* and the underlying substrate concentration u at two sites: in the first term by virtue of the additional space effect and in the third term by virtue of the effect of saturation on the tracer sequestration mechanism. Now examine the case in which tracer is introduced as a unit pulse at $x = 0$ and at a new time, $t = 0$. The initial conditions are

$$u^*(x, 0)=\frac{q_o}{Ar}\delta^*(x)=\frac{q_o}{ArW}\delta^*\left(\frac{x}{W}\right) \tag{17}$$

where q_o is the chemical amount of tracer injected, Ar is the cross-sectional area of the sinusoid, and $ArW = F_s$, the sinusoidal flow of tracer bearing fluid.

First, examine the case in which e_T/K_m is so small as to be insignificant. This will apply to ethanol, for instance, at all concentrations except those in the very lowest range (13). Define

$$A=\frac{(1+\beta+\gamma+\theta)}{(1+\beta)W}$$

and

$$B'=\frac{V_{max}\theta}{(1+\beta)W(u+K_m)}$$

Change the time variable using the relation $t' = t - Ax$. *Equation 16c* then becomes

$$\frac{du^*}{dx}+B'u^*=0 \tag{18}$$

The solution to this differential equation is

$$u^*(x, t')=C(t')e^{-\int_0^x B'df} \tag{19}$$

where $C(t')$ is the constant of integration and f is the dummy variable of the integration. Changing the variable of integration from x to u by use of the relation defined by *Eq. 8a*, we find

$$-\int_0^x B'df=\int_{u_o}^{u}\frac{dg}{g}=\ln\left(\frac{u}{u_o}\right)$$

where g is the dummy variable of the new integration. Then

$$u^*(x, t')=C(t')\frac{u}{u_o} \tag{20}$$

and because

$$u^*(0, t)=\frac{q_o}{F_s}\delta^*\left(\frac{x}{W}\right)$$

we find

$$u^*(x, t)=\frac{q_o}{F_s}\left[\frac{u}{u_o}\right]\delta^*\left[t-\frac{(1+\beta+\gamma+\theta)x}{(1+\beta)W}\right] \tag{21}$$

The linkage between the tracer kinetics and the concentration of the "mother substance" becomes explicit in this final solution. The tracer propagates as an impulse function, with a progressive reduction in area, which accurately reflects the uptake of the mother substance, the substance being traced. The velocity of the impulse, $(1+\beta)W/(1+\beta+\gamma+\theta)$, is diminished in relation to that of the reference red cells, W, by the blood-to-blood plus tissue distribution space ratio for the tracer.

Equation 21 can also be developed in an alternate but more explicit form. Consider, in this case, events at the outflow. Write *Eq. 9b* at $x = L$ but divide through by $\ln u_o - \ln u_L$ to obtain

$$K_m + \frac{u_o - u_L}{\ln u_o - \ln u_L} = \frac{V_{max}\theta}{(1+\beta)}\frac{L}{W}\frac{1}{\ln(u_o/u_L)}$$

but this is

$$\ln\left[\frac{u_o}{u_L}\right] = \frac{V_{max}\theta}{(1+\beta)(K_m+\hat{u})}\frac{L}{W}$$

and therefore

$$\frac{u_L}{u_o} = e^{-\frac{V_{max}\theta}{(1+\beta)(K_m+\hat{u})}\frac{L}{W}}$$

so that

$$u^*(L,t) = \frac{q_o}{F_s}e^{-\frac{V_{max}\theta}{(1+\beta)(K_m+\hat{u})}\frac{L}{W}} \cdot \delta^*\left[t - \frac{(1+\beta+\gamma+\theta)}{(1+\beta)}\frac{L}{W}\right] \quad (21a)$$

This equation will provide an appropriate description of the behavior of tracer whenever the incremental enzymic space is negligible (i.e., whenever it is too small to be perceptible).

Now let us examine the case in which the incremental enzymic space is finite. Again consider *Eq. 16c*, this time with finite values for e_T/K_m. The equation becomes linear in the two concentration extremes [these are important in the accompanying paper (13) in which the behavior of the straight-chain monohydric alcohols at the two extremes is explored]. The behavior of tracer at these extremes is as follows.

a) When $u \to 0$ the outflow of tracer from a single sinusoid after an impulse injection is

$$u^*(x,t) = \frac{q_o}{F_s}e^{-\frac{V_{max}\theta}{K_m(1+\beta)}\frac{x}{W}} \cdot \delta^*\left[t - \frac{(1+\beta+\gamma+\theta[1+e_T/K_m])}{(1+\beta)}\frac{x}{W}\right] \quad (22)$$

The velocity of propagation of tracer, $\{(1+\beta)/(1+\beta+\gamma+\theta[1+e_T/K_m])\}W$, is constant and the system behaves in a linear fashion. This asymptote is approached experimentally by carrying out tracer injection in the absence of preceding infusion of unlabeled substrate. When e_T/K_m is appreciable, the tracer impulse emerges at the outflow, reduced in area and delayed with respect to the outflow arrival of its appropriate reference (a substance with the same β, γ, and θ ratios that does not associate with the enzyme); when e_T/K_m is too small to be perceived, the labeled substance will emerge at the outflow at the same time as its appropriate reference.

b) When $u \to \infty$ the outflow of tracer from a single sinusoid after an impulse injection becomes

$$u^*(x,t) = \frac{q_o}{F_s}\delta^*\left[t - \frac{(1+\beta+\gamma+\theta)}{(1+\beta)}\frac{x}{W}\right] \quad (23)$$

The velocity of propagation of tracer, $[(1+\beta)/(1+\beta+\gamma+\theta)]W$, is again constant (and now is independent of enzyme concentration). The tracer propagates as a delayed wave, losing essentially none of its contained activity. It converges on the behavior of its ideal reference substance, a material flow limited in its distribution that has the same blood and tissue spaces of distribution and is not removed from the system.

Although the low and high concentration extremes are independent of tracee, the problem that presents is how to describe the intermediate case: when tracee concentration is neither low nor high with respect to the K_m. From general principles, we would again expect the tracer recovery to match the predicted bulk recovery. The problem that emerges is describing the velocity of propagation of the impulse. Insight can be gained by further developing the description of bulk behavior. *Equation 7b* can be written as a directional differential equation in the form

$$f(u)\frac{\partial u}{\partial t} + \frac{\partial u}{\partial x} + g(u) = 0$$

where

$$f(u) = \frac{(1+\beta+\gamma+\theta[1+e_T/\{u+K_m\}])}{(1+\beta)W}$$

and

$$g(u) = \frac{V_{max}\theta u}{(1+\beta)W(u+K_m)}$$

Recall that

$$du = \frac{\partial u}{\partial t}dt + \frac{\partial u}{\partial x}dx$$

so that

$$\frac{du}{dx} = \frac{\partial u}{\partial t}\frac{dt}{dx} + \frac{\partial u}{\partial x}$$

The partial differential equation can then be written as an ordinary differential equation

$$\frac{du}{dx} + g(u) = 0$$

in the direction

$$\frac{dt}{dx} = f(u)$$

This equation indicates that a concentration step function will propagate with the velocity

$$\frac{dx}{dt} = \frac{(1+\beta)W}{(1+\beta+\gamma+\theta[1+e_T/\{u+K_m\}])} \quad (24)$$

the steady state being established immediately because there are no barriers. A tracer impulse will, of course, propagate with the same velocity. Since the steady-state concentration profile $u(x)$ varies along the length, the velocity of a superimposed tracer impulse will also vary, increasing along the length with the decrease in concentration. The position of the impulse function in time is dictated by the concentration profile $u(x)$; it must be found by an appropriate set of numerical calculations. The variable velocity dx/dt has, of course, the two asymptotes already outlined above.

Tracer studies in the whole organ. Tracer studies carried out at the level of the whole organ potentially provide information concerning the whole ensemble of

sinusoidal transit times and, with this, the possibility of obtaining some information concerning the corresponding family of outflow bulk or tracee concentrations. Gaining insight into this matter has been complicated because, although outflow tracer values are immediately recorded and accessible to the investigator, the underlying arrays of venous tracee values that constitute the elements of the measurable mixed venous outflow concentration are inaccessible and hence can be gauged only by calculating these from outflow tracer values on the basis of relations such as those described by the above equations. If the concentrations from input to the various venous output values sweep across a significant range with respect to K_m, it might be expected that V_{max} and K_m estimates could be obtained from a single tracer experiment. If this does not happen the single tracer experiment will give insight only into a small part of the whole concentration range, and saturation effects will not be evident within the single tracer experiment but will be revealed by carrying out a set of repeated tracer experiments while steady-state input concentrations are varied across an appropriately broad range of concentrations. Because the requisite information at this level then cannot usually be obtained in an individual animal, many animals will usually need to be studied, and the experimental data set will contain not only the desired variation of tracer uptake with the underlying steady-state tracee concentration but also the variation encountered from animal to animal.

In applying the developments outlined above, it is necessary to use knowledge gained earlier concerning the relation between large- and small-vessel transit times in specific organs (15). In the liver, the organ on which we are focusing here, Goresky (8), analyzing a set of multiple-indicator dilution curves, found that after a common initial time the curves for labeled albumin, a group of extracellular reference substances (inulin, sucrose, and sodium), and labeled water could in each case be made to superimpose on the labeled red cell curve by decreasing the subsequent times along each curve by a single factor and compensatorily increasing its magnitudes by the inverse of the factor. The findings were interpreted to indicate the presence of a common large-vessel transit time (the common initial time) together with, for each diffusible label, that distribution of sinusoidal transit times resulting from flow-limited distribution of each into its corresponding extravascular space during flow along the sinusoid. In what follows we reconstruct these observations and use them to provide a basis for extending the single-sinusoidal modeling developed earlier to the whole organ.

The liver has a symmetry of structures such that lobular pathways have a virtually common length, L. The distribution of sinusoidal transit times will result chiefly from variations in sinusoidal velocity, W_s, across the various pathways. With these considerations in mind, define F_s as the flow in the local sinusoid; W_s as the corresponding velocity of propagation of red cells; F as the total flow through the liver; $n(L/W_s)d(L/W_s)$ as the proportion of sinusoids with transit times from (L/W_s) to $(L/W_s) + d(L/W_s)$, arising from the distribution of velocities in the sinusoids; $C^*(t')_{RBC}$ as the outflow fraction per milliliter profile for labeled red cells (13); $h(t)_{RBC}$ as the transport function or probability density function of the system for labeled red cells; and t_o as the common large-vessel transit time. We then find for labeled red cells (the vascular reference substance) that if $t' = t - t_o$

$$\begin{aligned} F C^*(t')_{RBC} &= h(t')_{RBC} \\ &= \int_{(L/W_s)_{min}}^{L/W_s} F_s(\tau)\delta^*(t' - \tau)n(\tau)\,d\tau \\ &= F_s(t')n(t') \end{aligned} \quad (25)$$

where τ is the dummy variable of integration and $(L/W_s)_{min}$ is the minimum sinusoidal transit time. Now consider the behavior of a flow-limited, second-reference substance. In a metabolic uptake study, in which the cellular surface presents no barrier to entry of substrate, labeled water is an appropriate second-reference substance because it marks out the parenchymal cell water space. In this case, if $C^*(t')_{THO}$ is the outflow fraction per milliliter profile for labeled water and $h(t)_{THO}$ is the probability density function of the system for labeled water, we find

$$\begin{aligned} &F C^*(t')_{THO} \\ &\quad = h(t')_{THO} \\ &\quad = \int_{(L/W_s)_{min}}^{L/W_s} F_s(\tau) \\ &\qquad \cdot \delta^*\left[t' - \frac{(1+\beta+\gamma+\theta)}{(1+\beta)}\tau\right] n(\tau)\,d\tau \\ &\quad = \frac{h\left[\dfrac{(1+\beta)t'}{(1+\beta+\gamma+\theta)}\right]_{RBC}}{\dfrac{(1+\beta)}{(1+\beta+\gamma+\theta)}} \end{aligned} \quad (26)$$

where θ is now the parenchymal cell-to-sinusoidal plasma space ratio for labeled water and τ is again the dummy variable of integration. Transforming the labeled water curve in the manner instructed by *Eq. 26*, one can find optimal estimates of t_o and of $(1 + \beta + \gamma + \theta)/(1 + \beta)$, the total-to-sinusoidal space ratio for labeled water.

The question that then emerges is how to analyze outflow dilution curves for a tracer freely entering both red cells and liver cells but removed by an enzymic mechanism when tracee is in a steady state. The general answer would be to calculate an outflow tracer curve from that for an appropriate reference, using the input tracee concentration and an approach corresponding to that outlined above, optimizing V_{max} and K_m values for the tracee until a close fit between calculated and experimental data is achieved. The transcendental nature of *Eq. 9*, which must be used in the evaluation of the elemental *Eq. 21* or its more complicated analogues, makes this straightforward approach somewhat difficult. Moreover, the values for V_{max} and K_m obtained by this approach would not be expected to be very accurate unless inflow and underlying elemental outflow tracee concentrations span a large range on either side of the

K_m value within the single experiment. When the concentrations from input to output across the various transit time pathways sweep across a very narrow proportion of the concentration range with respect to the K_m, saturation effects will not be expected to be visible within the tracer curve; at the experimental level the kinetics will appear to be linear.

Let us examine the linear case, which corresponds to *Eq. 21a*, in which the incremental space effect is not perceptible at the experimental level [this corresponds to what was found in experimental explorations with labeled ethanol, where an enzymic space effect was present only at radiochemical levels of concentration (13); the estimated space of distribution did not otherwise vary from that for labeled water]. At the level of the outflow profile from the whole liver, we would expect for the more general alcohol case (where θ' may not be equal to θ for labeled water) that

$$FC^*(t')_{Alc} = \int_{(L/W_s)_{min}}^{L/W_s} F_s(\tau)\, e^{-\left[\frac{V_{max}\theta'}{(1+\beta)(\hat{u}+K_m)}\right]\tau} \cdot \delta^*\left[t' - \frac{(1+\beta+\gamma+\theta')}{(1+\beta)}\tau\right] n(\tau)\,d\tau \quad (27)$$

$$= e^{-\left[\frac{V_{max}\theta'}{(1+\beta+\gamma+\theta')(\hat{u}+K_m)}\right]t'} h(t')_{Ref\,2}$$

where $C^*(t)_{Alc}$ is the outflow fraction per milliliter profile for labeled alcohol and $h(t)_{Ref\,2}$ is the transport function of the reference corresponding to the labeled alcohol. When $\theta' = \theta$, the second-reference curve, $h(t')_{Ref\,2}$, will correspond to that of labeled water, and *Eq. 27* will correspond to the behavior found for labeled ethanol. The uptake rate constant in this equation deserves further examination. It may be expressed in the form $V_{tot}/(\hat{u} + K_m)$, where $V_{tot} = V_{max}\,\theta'/(1 + \beta + \gamma + \theta')$. The value of $\hat{u}$ that one would expect to need to insert in this rate constant corresponds to the t' or L/W_s value along the curve. If, however, the family of venous tracee concentrations spans only a small range with respect to the K_m within the single-dilution curve, the uptake rate constant will appear to correspond to only a single value. In that event, the two parameters one would necessarily seek to optimize on the basis of this equation are the space ratio $(1 + \beta + \gamma + \theta')/(1 + \beta)$ and the apparently single-valued uptake rate constant. Mechanistically, this will involve generating a set of second-reference curves with varied θ' values and finding the rate constant that, with some particular curve, gives a best fit (according to the above equation) to the labeled alcohol curve. For labeled ethanol and labeled water, space ratio values were found to be the same for all measurable input concentrations of bulk ethanol. The labeled water curve could then be utilized as a second-reference curve in the analysis of the data. The uptake rate constant for ethanol, with the dimensions $ml \cdot s^{-1} \cdot (ml\ total\ space\ of\ distribution)^{-1}$, was found to diminish with bulk concentration across the set of experiments. Within a particular experiment, *Eq. 27* indicates that the relation between the labeled water and labeled ethanol curves will be described by the relation

$$\ln\left[\frac{C^*(t')_{THO}}{C^*(t')_{Eth}}\right] = \frac{V_{tot}}{(\hat{u} + K_m)}\,t' \quad (28)$$

A plot of the natural logarithm of the ratio of the labeled water to labeled ethanol outflow fractions per milliliter would be expected to give a line that bows upward with time if the underlying bulk $\hat{u}$ value were to decrease significantly with respect to the K_m along the curve and to give a rising straight line with constant slope if it does not. Experimentally, the slope was found to remain constant and not to increase with time (13).

In this particular case it becomes possible to proceed rather simply to the determination of the parameters characterizing the enzymic sequestration mechanism. If R is the uptake or sequestration rate constant determined within a particular experiment, the family of R values obtained across a range of steady-state experiments with varying alcohol values will be

$$R = \frac{V_{tot}}{(\hat{u} + K_m)} \quad (29)$$

where V_{tot} is the maximal rate at which bulk substrate can be removed by the enzyme at saturation per milliliter total liver space. At radiochemical concentrations the uptake rate constant will have the value V_{tot}/K_m and, as the underlying tracee concentration is increased, the rate constant will be expected to diminish. The form of the relation corresponds to what is found experimentally. Values for V_{tot} and K_m are found by fitting *Eq. 29* in a least-squares fashion to the relation between the tracer uptake rate constant and the underlying logarithmic average bulk substrate concentration. The relation resolves a dilemma alluded to earlier by Goresky et al. (12): deciding how to relate a sequestration rate constant to underlying substrate concentrations when these progressively diminish from input to outflow. The appropriate choice of concentration is made clear by the equation.

Underlying Steady State When There Is One Barrier in System

For substances not penetrating cell membranes freely in the liver, a single effective barrier will be present between blood and the site of metabolic removal. For substances such as these, which will normally be distributed into the extracellular space of the liver (the space of Disse) in a flow-limited fashion, a resistance to transfer will be present at the cell surface. Where there is an effective intracellular removal process in addition, a concentration difference will develop across the cell membrane, and this will be present even in the steady state. This set of phenomena is important, but it has not been widely recognized. It has been, for instance, totally neglected in the otherwise careful analysis carried out by Keiding et al. (20) of saturation effects in the elimination of galactose by the perfused pig liver.

Assume that there is a barrier at the liver cell membrane (between the space of Disse and the liver cell contents) and that there is flow-limited distribution into the Disse space as before. Further assume that the substance does not enter red cells (i.e., $\beta = 0$). In this

development, now let the intracellular concentration be $z(x, t)$.

The partial differential equation describing conservation in this system, as a function of $u(x, t)$ and $z(x, t)$, developed in analogy to *Eqs. 7*, is

$$(1 + \gamma)\frac{\partial u}{\partial t} + W\frac{\partial u}{\partial x} + \theta\frac{\partial z}{\partial t} + \frac{V_{max}\,\theta z}{z + K_m} = 0 \qquad (30)$$

or

$$\frac{(1 + \gamma)}{W}\frac{\partial u}{\partial t} + \frac{\theta}{W}\frac{\partial z}{\partial t} + \frac{\partial u}{\partial x} + \frac{V_{max}\,\theta z}{W(z + K_m)} = 0 \qquad (30a)$$

In this development we have assumed that e_T/K_m is small, so that the extra-space effect need not be considered in concrete fashion. The equation describing the exchange of material between the plasma and intracellular spaces is

$$\frac{\partial z}{\partial t} = k_1 u - k_2 z - \frac{V_{max}\,z}{z + K_m} \qquad (31)$$

where k_1 and k_2 are membrane transfer rate constants, with the dimensions $ml \cdot s^{-1} \cdot (ml\ intracellular\ space)^{-1}$.

Let the initial condition again be a step input of magnitude u_o beginning at *time* 0

$$u(x, 0) = u_o\,S(x)$$

where $S(x)$ is a step function at the origin. Assess the response in the steady state when $t \to \infty$ or $\partial u/\partial t = \partial z/\partial t = 0$. The solution to this case will provide a description of the lobular gradients in the steady state. *Equations 30* and *31* become

$$\frac{du}{dx} + \frac{V_{max}\theta z}{W(z + K_m)} = 0 \qquad (32)$$

and

$$k_1 u = z\left(k_2 + \frac{V_{max}}{z + K_m}\right) \qquad (33)$$

If we multiply *Eq. 32* by k_1 and differentiate *Eq. 33*, we find, by equating the two resulting expressions for $k_1 du/dx$, the following expression in z

$$\frac{1}{V_{max}}\left(\frac{k_2(z + K_m)^2 + V_{max}K_m}{z(z + K_m)}\right)dz = -k_1\theta\frac{dx}{W} \qquad (34)$$

which, on decomposition by partial fractions and integration, becomes

$$\frac{(k_2K_m + V_{max})}{V_{max}}\ln z - \ln(z + K_m) + \frac{k_2 z}{V_{max}} = -k_1\theta\frac{x}{W} + \text{constant} \qquad (35)$$

or

$$\frac{z^{\frac{k_2K_m + V_{max}}{V_{max}}}}{(z + K_m)}\,e^{\frac{k_2}{V_{max}}z} = \text{constant}\;e^{-k_1\theta\frac{x}{W}} \qquad (35a)$$

At $x = 0$, $z = z_o$; thus

$$\text{constant} = \frac{z_o^{\frac{k_2K_m}{V_{max}}+1}}{(z_o + K_m)}\,e^{\frac{k_2}{V_{max}}z_o}$$

so that

$$\left(\frac{z_o + K_m}{z + K_m}\right)\left(\frac{z}{z_o}\right)^{\frac{k_2K_m}{V_{max}}+1} e^{-\frac{k_2}{V_{max}}(z_o - z)} = e^{-k_1\theta\frac{x}{W}} \qquad (35b)$$

Now we must find the value for z_o. Since, at $x = 0$, $u = u_o$ and $z = z_o$, these values can be substituted in *Eq. 33*. From this substitution we find

$$z_o^2 + \left(\frac{k_2K_m + V_{max} - k_1u_o}{k_2}\right)z_o - \frac{k_1}{k_2}K_mu_o = 0 \qquad (36)$$

For a given value of u_o and with given values of the other parameters in this equation, the quadratic can be solved for z_o. The value needed is the real and positive root.

With this value, the challenge becomes that of solving *Eq. 35b* for z at various values of x/W. No simple algebraic method of solution is available, inasmuch as the equation is transcendental in the unknown. The solution to the equation can be found numerically, however, by choosing a value for z, substituting this in the function of z formed by the difference of the two sides of *Eq. 35b*, and improving the resulting estimate of z by the secant method (22) until the function becomes equal to zero. Given the value of z at a particular x/W, the corresponding value of u can be found from *Eq.* 33.

The limiting asymptotic extremes are again of particular interest.

a) If z_o and $z \ll K_m$, then $z_o + K_m \to K_m$ and $z + K_m \to K_m$. In this extreme, *Eq. 32* becomes

$$\frac{du}{dx} = -\frac{V_{max}\theta z}{K_mW} \qquad (37)$$

and *Eq. 33* becomes

$$k_1 u = (k_2 + V_{max}/K_m)z \qquad (38)$$

so that

$$\frac{du}{dx} + \frac{V_{max}\theta k_1}{WK_m(k_2 + [V_{max}/K_m])}u = 0$$

Then

$$u = u_o e^{-\left[\frac{k_1[V_{max}/K_m]\theta}{k_2 + [V_{max}/K_m]}\right]\frac{x}{W}} \qquad (39)$$

and

$$z = \frac{k_1}{\{k_2 + [V_{max}/K_m]\}}u \qquad (40)$$

Each concentration decreases exponentially as a function of the length, and there is a constant ratio between u and z at each point along the length from entrance to exit.

This solution corresponds in form to the set of steady-state profiles predicted by Goresky et al. (11) in their exploration of the limiting effects of the cell membrane on the disposal of galactose by the liver (in this exploration, sequestration was considered to take place in a linear or nonsaturating fashion). The parameter V_{max}/K_m in this linear asymptotic extreme corresponds to their linearized intracellular sequestration rate constant k_3. As

zero galactose concentration is approached, the limiting value of this sequestration constant will be expected to provide a good numerical estimate of V_{max}/K_m.

b) If z_o and $z \gg K_m$, then $z_o + K_m \rightarrow z_o$ and $z + K_m \rightarrow z$. In this extreme, *Eq.* 32 becomes

$$\frac{du}{dx} = -\frac{V_{max}\theta}{W}$$

so that

$$u = u_o - V_{max}\theta \frac{x}{W} \tag{41}$$

In this extreme, we also find from *Eq. 31* that

$$\begin{aligned} z &= \frac{k_1}{k_2} u - \frac{V_{max}}{k_2} \\ &= \frac{k_1 u_o - V_{max}}{k_2} - V_{max}\theta \frac{k_1}{k_2} \frac{x}{W} \\ &= z_o - V_{max}\theta \frac{k_1}{k_2} \frac{x}{W} \end{aligned} \tag{42}$$

In each phase (sinusoidal plasma and liver cells), there is a linear decline in concentration along the length, which is independent of plasma concentration. Rather, the decline is dependent on the maximal removal rate and the velocity of flow. When $k_1/k_2 = 1$ (i.e., if the system were predicted to behave in a nonconcentrative fashion in the absence of a removal process), z will differ from u at each point along the length by V_{max}/k_2.

The experimental data of Goresky et al. (11) provide a set of numerical parameters that can be used to model the expected sinusoidal and cellular lengthwise concentration profiles in the liver when galactose is being steadily infused in such a fashion that input concentrations are stable. The data indicate that, over the usually encountered concentration range for galactose, the sequestration process saturates quickly, whereas the membrane transfer process remains virtually proportional to concentration. In Figs. 3 and 4, the expected steady-state profiles, calculated with *Eqs. 33* and *35b*, are displayed for sinusoids with vascular (red cell) transit times of 2 and 5 s. At the lowest galactose concentration, both the relative decrease in concentration from input to output and the relative drop in concentration across the cell membrane are large.

Increase in the input galactose concentration diminishes both relative effects by saturating the uptake mechanism. Increase in the transit time (i.e., slowing the flow) increases the net uptake of galactose at all concentrations. Because there is a large heterogeneity of transit times in the liver, it is appropriate to illustrate the systematic kind of effects that will be found across a spectrum of sinusoidal transit times. The effect of varying the transit time on the ratio of output to input concentration over a wide range of input concentrations is displayed in Fig. 5 for transit times of 2, 5, and 10 s. It is evident that the transit time exerts a major influence on the net uptake of galactose, an effect that is especially marked in the lower concentration range.

Tracer Studies in Steady State When There Is a Single Barrier in System

In this instance the response becomes markedly different from the case in which there is no barrier in the system. The barrier introduces a whole new set of effects on tracer kinetics.

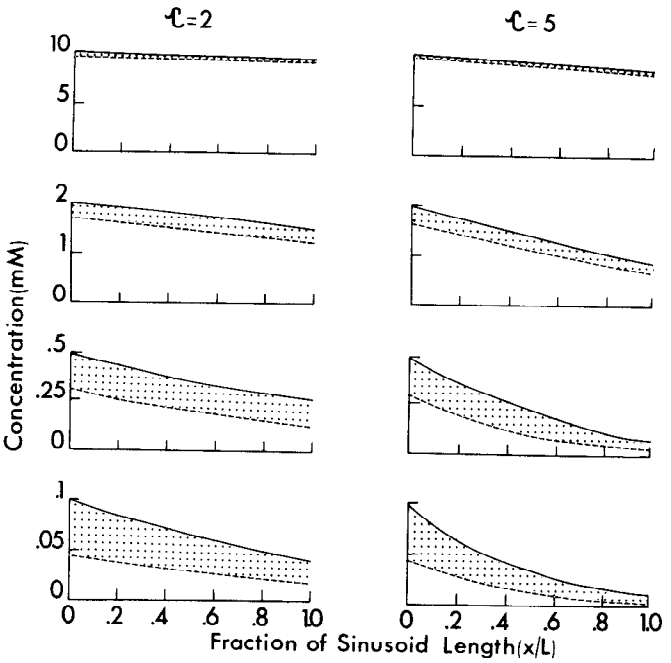

FIG. 3. Steady-state galactose concentrations in vascular (*solid line*) and cellular (*dashed line*) compartments as a function of sinusoidal length. Concentration drop between vascular and cellular compartments (difference between solid and dashed lines) is shaded to provide emphasis. Input sinusoidal concentrations are those recorded at $(x/L) = 0$. *Left hand panels*: mean sinusoidal transit time (τ) of 2 s; *right-hand panels*: mean transit time of 5 s. Characteristic parameters utilized for the calculations were those estimated by Goresky et al. (11): a maximal removal rate of 0.05 mmol·s^{-1}·l^{-1} and a K_m of 0.25 mM. Parameter θ was given value 5.5, and γ was given value 1.0 (these were averages for data set). Rate constants k_1 and k_2 were set equal to 0.14·s^{-1} (these were average values found over the concentration range across which saturation of sequestration process occurred).

Once again, consider a tracer experiment in a system that is in steady state as to concentration of the unlabeled parent material. Let u^* and z^* represent tracer material in the vascular and cellular compartments; u' and z', unlabeled material in the vascular and cellular compartments; and u and z, the sum of the respective labeled and unlabeled species. Then, by analogy with *Eqs. 8* and *16*, the equation describing conservation in the system is

$$\begin{aligned} (1+\gamma)\frac{\partial(u'+u^*)}{\partial t} + W\frac{\partial(u'+u^*)}{\partial x} \\ + \theta\frac{\partial(z'+z^*)}{\partial t} + \frac{V_{max}\theta(z'+z^*)}{(z'+z^*+K_m)} = 0 \end{aligned} \tag{43}$$

And, by analogy with *Eq. 16c*, the equation describing label behavior in the tracer case when $x' = x/W$ is

$$\begin{aligned} (1+\gamma)\frac{\partial u^*}{\partial t} + \frac{\partial u^*}{\partial x'} + \theta\frac{\partial z^*}{\partial t} \\ + V_{max}\theta\left(\frac{z^*}{z+K_m}\right) = 0 \end{aligned} \tag{44}$$

From *Eq. 31*, the rate equation describing exchange across the barrier is in the steady state

$$\begin{aligned} \frac{\partial(z'+z^*)}{\partial t} = k_1(u'+u^*) - k_2(z'+z^*) \\ - \frac{V_{max}(z'+z^*)}{(z'+z^*+K_m)} = 0 \end{aligned} \tag{45}$$

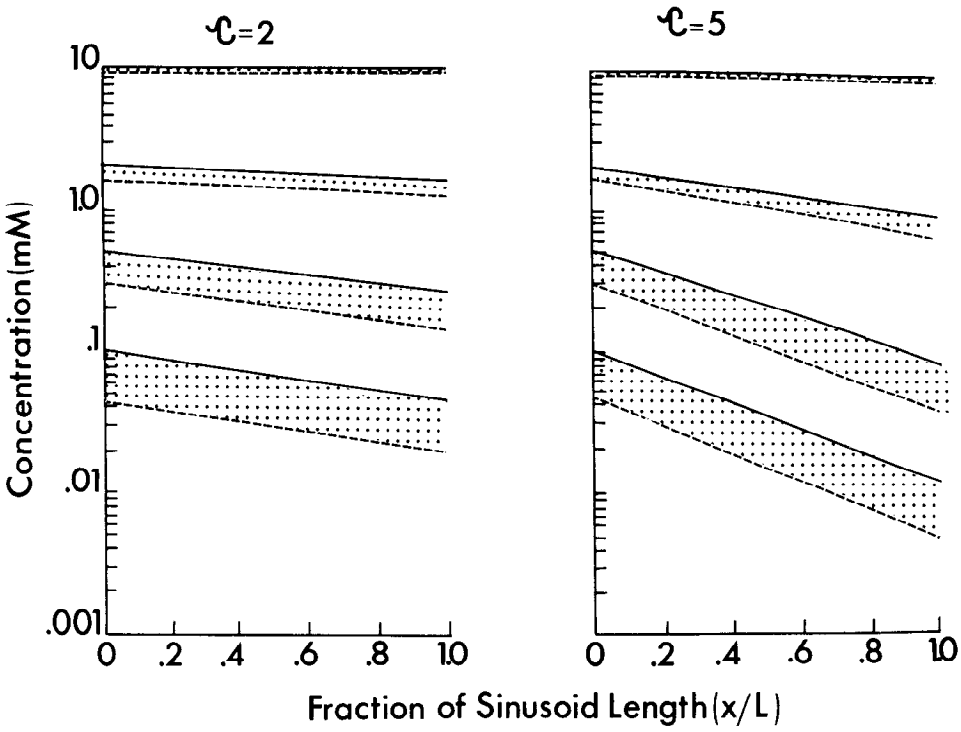

FIG. 4. Data from Fig. 3 plotted against a continuous logarithmic scale. Concentration drop between vascular and cellular compartments is shaded. Relative alteration in concentration-space profiles, with change in input concentration and change in sinusoidal mean transit time, is made obvious with this kind of display.

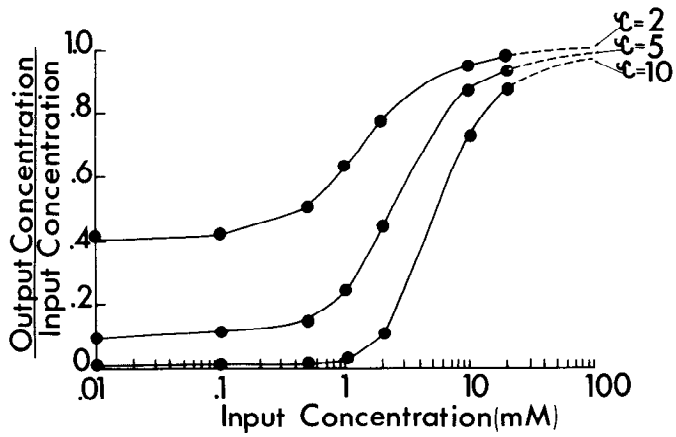

FIG. 5. Change in ratio of output concentration to input concentration as a function of both sinusoidal mean transit time and input concentration. In low concentration range, proportion of galactose surviving at outflow very obviously increases as flow increases, as sinusoidal transit time is shortened. At high concentration extreme, a large proportion of galactose emerges at outflow. Relative transit time effect becomes small. Parameter values utilized to generate figure were those used to generate Figs. 3 and 4.

Dealing with the saturation term in the same manner as previously, we find

$$\frac{\partial z^*}{\partial t} = k_1 u^* - k_2 z^* - \frac{V_{max} z^*}{(z + K_m)} \qquad (46)$$

These equations are to be solved in the steady state after a step infusion of the parent substance (*Eqs. 32* and *33*). The last terms of *Eqs. 44* and *46* provide the linkage with the underlying steady-state lengthwise concentrations u and z. If the tracer is introduced at the origin as an impulse function (*Eq. 17*), the initial conditions become

$$u^*(x', 0) = \frac{q_o \delta^*(x')}{F_s}$$

where q_o is the chemical amount of tracer injected and $z^*(x', 0) = 0$.

Now carry out the Laplace transformation on *Eqs. 44* and *46*, utilizing the following definitions

$$\bar{U}(x, s) = \int_0^\infty u^*(x, t) e^{-st}\, dt$$

and

$$\bar{Z}(x, s) = \int_0^\infty z^*(x, t) e^{-st}\, dt$$

The equations become

$$s(1 + \gamma)\bar{U} - (1 + \gamma)\frac{q_o \delta^*(x')}{F_s} + \frac{d\bar{U}}{dx'} + \left(s\theta + \frac{V_{max}\theta}{(z + K_m)}\right)\bar{Z} = 0 \qquad (47)$$

and

$$s\bar{Z} = k_1 \bar{U} - k_2 \bar{Z} - \frac{V_{max}\bar{Z}}{(z + K_m)} \qquad (48)$$

When the expression for $\bar{Z}$ resulting from *Eq. 48* is substituted into *Eq. 47*, we find

$$\frac{d\bar{U}}{dx'} + \bar{U}\left[s(1 + \gamma) + \frac{k_1\theta\{s + V_{max}/(z + K_m)\}}{s + k_2 + V_{max}/(z + K_m)}\right] = \frac{(1 + \gamma)q_o}{F_s}\delta^*(x')$$

or

$$\frac{d\bar{U}}{dx'} + \bar{U}\left[s(1 + \gamma) + k_1\theta - \frac{k_1\theta k_2}{s + k_2 + V_{max}/(z + K_m)}\right] = \frac{(1 + \gamma)q_o}{F_s}\delta^*(x') \qquad (49)$$

The solution to this equation must take into account the fact that the steady-state profile of z is a function of x'.

In this instance we can best arrive at an understanding of the behavior of the solution if we first investigate the two extremes: $z \ll K_m$ (the case in which the z concentration falls exponentially along the length) and $z \gg K_m$ (the case in which the z profile falls linearly along the length). If we set

$$b = k_2 + V_{max}/(z + K_m) \tag{50}$$

then we find

$$b = k_2 + V_{max}/K_m \qquad z \ll K_m \tag{50a}$$

and

$$b = k_2 \qquad z \gg K_m \tag{50b}$$

At both extremes b becomes independent of z. The lumped parameter describing the removal of tracer, $V_{max}/(z + K_m)$, will vary from a maximum, V_{max}/K_m, when $z \ll K_m$, to zero, when $z \gg K_m$. The parameter b will vary from a maximum, $k_2 + V_{max}/K_m$, to a minimum, k_2, as tracer experiments are carried out in the experimental situation in which the load of mother substances varies from zero to very large.

The transform for the two solutions is found to be

$$\bar{U}(x, s) = (1 + \gamma)\frac{q_o}{F_s} e^{-(1+\gamma)sx' - k_1\theta x' + \frac{k_1\theta k_2 x'}{s+b}} \tag{51}$$

The solutions for the two asymptotic extremes, in which b is independent of z, have previously been described by Goresky et al. (10, 11). They are embodied in the equation

$$\begin{aligned} u^*(x, t) &= \frac{q_o}{F_s} e^{-\left(k_1\theta\frac{x}{W}\right)}\delta\left\{t - (1 + \gamma)\frac{x}{W}\right\} + \frac{q_o}{F_s} e^{-b\left\{t-(1+\gamma)\frac{x}{W}\right\}} \\ &\cdot e^{-\left(k_1\theta\frac{x}{W}\right)} \sum_{n=1}^{\infty} \frac{\left(k_1\theta k_2 \frac{x}{W}\right)^n \left\{t - (1 + \gamma)\frac{x}{W}\right\}^{n-1}}{n!(n-1)!} \\ &\cdot S\left\{t - (1 + \gamma)\frac{x}{W}\right\} \\ &= \frac{q_o}{F_s} e^{-\left(k_1\theta\frac{x}{W}\right)}\delta\left\{t - (1 + \gamma)\frac{x}{W}\right\} \\ &+ \frac{q_o}{F_s} e^{-b\left\{t-(1+\gamma)\frac{x}{W}\right\}} e^{-\left(k_1\theta\frac{x}{W}\right)} \sqrt{\frac{k_1\theta k_2 \frac{x}{W}}{t - (1 + \gamma)\frac{x}{W}}} \\ &\cdot I_1\left[2\sqrt{k_1\theta k_2 \frac{x}{W}\left\{t - (1 + \gamma)\frac{x}{W}\right\}}\right] \\ &\cdot S\left\{t - (1 + \gamma)\frac{x}{W}\right\} \end{aligned} \tag{52}$$

where $I_1(p)$ is a first-order modified Bessel function of argument p. The tracer outflow response consists of two parts: a damped impulse function emerging at the time $t = (1 + \gamma)x/W$ and a later spread-out-in-time second component that represents the tracer returning from the liver cells to the circulation. When $b = k_2 + V_{max}/K_m$ the area under the returning component will be diminished to a maximum extent (not all of the tracer will be recovered in the outflow), and when $b = k_2$ the outflow recovery will be complete. These are the two asymptotes.

The corresponding expressions for $z^*(x, t)$ are

$$\begin{aligned} z^*(x, t) &= k_1\frac{q_o}{F_s} e^{-b\left\{t-(1+\gamma)\frac{x}{W}\right\}} e^{-\left(k_1\theta\frac{x}{W}\right)} \\ &\cdot \sum_{n=0}^{\infty} \frac{\left(k_1\theta k_2 \frac{x}{W}\right)^n \left\{t - (1 + \gamma)\frac{x}{W}\right\}^n}{n!n!} \\ &\cdot S\left\{t - (1 + \gamma)\frac{x}{W}\right\} \\ &= k_1\frac{q_o}{F_s} e^{-b\left\{t-(1+\gamma)\frac{x}{W}\right\}} e^{-\left(k_1\theta\frac{x}{W}\right)} \\ &\cdot I_o\left[2\sqrt{k_1\theta k_2 \frac{x}{W}\left\{t - (1 + \gamma)\frac{x}{W}\right\}}\right] \\ &\cdot S\left\{t - (1 + \gamma)\frac{x}{W}\right\} \end{aligned} \tag{53}$$

where $I_o(p)$ is a modified zero-order Bessel function of argument p. In this case there is no impulse function. The profile in space and time evolves after the arrival of the impulse function, which is propagating with the velocity $W/(1 + \gamma)$ in the expanded sinusoidal space.

Now return to *Eq. 49*, which describes the complete case. First, solve the homogeneous equation. Find

$$\ln \bar{U} + (1 + \gamma)sx' + k_1\theta x' - \int_0^{x'} \frac{k_1\theta k_2 \mathrm{d}g}{(s + k_2) + V_{max}/(z + K_m)} = \text{constant} \tag{54}$$

where g is the dummy variable of the integration. The inverse transform will not be able to be evaluated unless the integral can be evaluated.

Two approaches can be used to find the solution to the problem. The exact solution to the problem can be sought. To approach this we use the relation

$$\mathrm{d}x' = \frac{\mathrm{d}x'}{\mathrm{d}z}\mathrm{d}z \tag{55}$$

and the expression for $\mathrm{d}x'/\mathrm{d}z$ from *Eq. 34*. We find

$$\begin{aligned} -\int_0^{x'} \frac{k_1\theta k_2 \mathrm{d}g}{s + k_2 + V_{max}/(z + K_m)} \\ = \frac{k_2}{V_{max}} \int_{z_o}^{z(x')} \left[\frac{k_2(j + K_m)^2 + V_{max}K_m}{(s + k_2)(j + K_m) + V_{max}}\right]\frac{\mathrm{d}j}{j} \end{aligned} \tag{56}$$

where j is now the dummy variable of integration in the right-hand expression. This expression can be integrated and the resulting transform for $\bar{U}$ can be inverted either analytically or numerically, as suggested by Forker and

Luxon (5). It is difficult to perceive the form of the outflow profile, if one uses this approach.

We have therefore explored the Laplace transform of the solution further in search of an approximate solution that can be related to the two asymptotic extremes outlined above. First, set the constant in *Eq. 54* to ln K. Then

$$\bar{U}(x', s) = K\, e^{-(1+\gamma)sx' - k_1\theta x' + \int_0^{x'} \frac{k_1\theta k_2 \mathrm{d}g}{(s+k_2)+V_{max}/(z+K_m)}} \tag{57}$$

For the complete solution, we find by integrating *Eq. 49* from $x' = -\epsilon$ to $x' = \epsilon$ that

$$K = \frac{(1+\gamma)}{F_s} q_o S(x')$$

where $S(x')$ is a step function at $x/W = 0$. We must solve the expression

$$\bar{U}(x', s) = \frac{(1+\gamma)}{F_s} q_o S(x') e^{-(1+\gamma)sx' - k_1\theta x' + \int_0^{x'} \frac{k_1\theta k_2 \mathrm{d}g}{(s+k_2)+V_{max}/(z+K_m)}} \tag{58}$$

Now resolve the integral in the exponent on the right-hand side by parts. Find

$$\int_0^{x'} \frac{k_1\theta k_2 \mathrm{d}g}{s + k_2 + V_{max}/(z + K_m)} = \frac{k_1\theta k_2 g}{s + k_2 + V_{max}/(z + K_m)} \Bigg|_0^{x'} - k_1\theta k_2 \int_{z_0}^{z(x')} x' \mathrm{d}\left(\frac{1}{s + k_2 + V_{max}/(j + K_m)}\right) \tag{59}$$

where j is the dummy variable of integration in the right-hand term. Thus

$$\bar{U}(x, s) = \frac{(1+\gamma)}{F_s}\left[e^{-(1+\gamma)sx' - k_1\theta x' + \frac{k_1\theta k_2 x'}{s+k_2+V_{max}/(z+K_m)}}\right] \times e^{-k_1\theta k_2 \int_{z_0}^{z(x')} x' \frac{\mathrm{d}}{\mathrm{d}j}\left(\frac{1}{s+k_2+V_{max}/(j+K_m)}\right)\frac{\mathrm{d}j}{\mathrm{d}x'}\mathrm{d}x'} \tag{60}$$

The expression in the large square brackets, together with the initial weight factor, comprises the dominant part of the solution, because this recovers the transform given by *Eq. 51* for the two limits, $z \ll K_m$ and $z \gg K_m$, whereas the last term of the solution, outside the large square brackets, may be regarded as a correction factor. In the two extremes, $z \ll K_m$ and $z \gg K_m$, the correction factor becomes unity. In the intermediate range the correction term will have some effect, but it will be expected to be small in magnitude. We therefore expect the inverse of the dominant term to provide a solution for $u^*(x, t)$ closely approximating the complete one. The approximate solutions for $u^*(x, t)$ and $z^*(x, t)$ arising from this are given by *Eqs. 52* and *53*, with the expression for b now becoming

$$b = k_2 + V_{max}/(z + K_m) \tag{61}$$

The saturation effect in each equation is at the level of the exponent in the solution that incorporates the parameter b. Now let

$$k_3 = \frac{V_{max}}{z + K_m} \tag{62}$$

and consider a single-dilution experiment. If z does not sweep through a large concentration range with respect to K_m, in the single experiment k_3 will appear to be constant within that experiment. This is what Goresky et al. (11) found in their analysis of tracer galactose experiments carried out against steady-state background concentrations. The problem once again becomes that of choosing the single value of z most representative of events in the single experiment. Although the reason for the choice cannot be formulated so clearly as it was for *Eq. 29*, it once again appears appropriate to utilize the logarithmic average concentration $\hat{z}$ for each experiment in this equation in order to optimize values for V_{max} and K_m over a whole data set. The values for $\hat{z}$, as such, are inaccessible at the experimental level. Only inflow and mixed venous outflow values for u will be available. If our assumption of the relative invariance of k_3 within a single experiment is valid, however, an average $\hat{z}$ can be calculated from $\hat{u}$, utilizing the relation

$$\hat{z} = \frac{k_1}{k_2 + k_3}\hat{u} \tag{63}$$

by analogy with *Eqs. 39* and *40*.

We now use the approximation equation to explore the expected behavior of tracer galactose when the input concentration for a liver sinusoid is set at various levels by a preceding steady infusion of bulk galactose. The tracer outflow profiles expected in response to an impulse injection of tracer galactose are shown in Fig. 6. In each instance, the outflow profile consists of two parts: a throughput pulse, reduced in magnitude by cell entry, and a trailing reentry profile, the result of return to the vascular space. Figure 6 depicts, in each instance, both the profile expected if all of the material returned to the circulation and the profile for returning the material in the presence of the sequestration process. The area between the two is shaded for emphasis. When the galactose concentration is zero, the tracer sequestration is a maximum. As the galactose concentration is raised, the proportion of tracer sequestered is progressively diminished, so that at very high concentrations the sequestration effect becomes vanishingly small. When the transit time is larger, the proportion of tracer emerging in the throughput pulse is diminished and that entering the liver cells is increased. A transit time effect is also evident at the level of the returning material. When the activity of the sequestrating process is large, the proportion of the activity returning in the trailing profile is smaller at larger transit times. A larger proportion of the total activity has been sequestered. When the activity of the sequestration process is small, the effect disappears.

In calculating the profiles for Fig. 6 with the approximation equation, we utilized the expression for b provided by *Eq. 61* and inserted a $\hat{z}$ value for z in this equation, based on z values at inflow and outflow, and calculated on the basis of *Eqs. 35* and *36*. If tracer traces bulk and if the approximation equation is reasonably

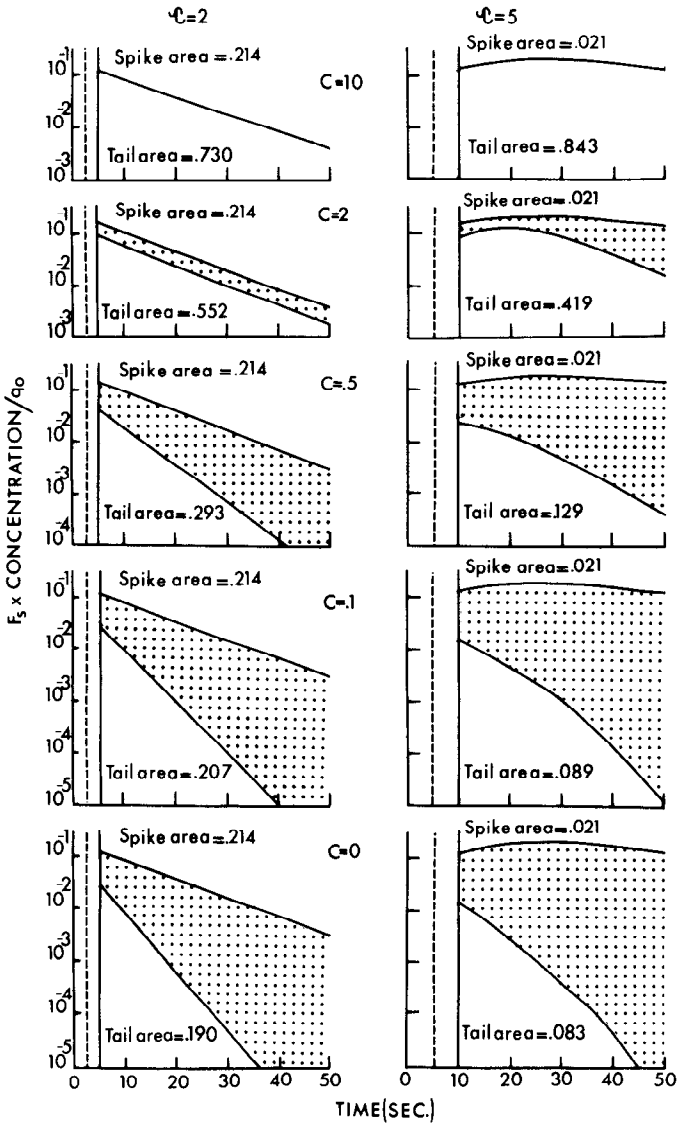

FIG. 6. Tracer outflow profiles expected in response to an impulse input of tracer galactose when bulk galactose concentration has been set at various levels by steady infusion. Values for V_{max}, K_m, and θ are those utilized to generate steady-state profiles in Fig. 3. Other parameters used in these calculation were $k_1 = k_2 = 0.14 \cdot s^{-1}$ and $\gamma = 1.0$. Underlying steady-state input galactose concentrations (C, mM) are listed in middle of figure. Output displayed is normalized single-sinusoidal transport function, which consists of a damped impulse function and a following tailing. Both tailing that could have been expected in absence of sequestration (*upper line*) and tailing that occurred in presence of sequestration (*lower line*) are shown. It is difficult to display an impulse function, which theoretically has an infinitely large magnitude and an infinitesimally short duration. In this illustration we have used a vertical line at appropriate time and indicated associated area by the term spike area, when recovery differs from unity. Area of trailing reentry profile is given as a tail area. By definition sum of spike area and area under upper trailing profile is unity. Sum of spike area and area under lower trailing profile defines tracer outflow recovery in presence of sequestration process. Area between two curves, uptake effect, is shaded to provide emphasis. A dashed spike is placed on illustration at time vascular reference would have emerged.

accurate, the predicted outflow recovery of tracer, based on the calculated profiles, should closely approach the outflow recovery of bulk material, calculated from the steady-state profiles described by *Eqs. 33, 35,* and *36*. In Table 1 we have calculated relative galactose outflow recoveries for both bulk and tracer with the parameters utilized to generate Figs. 3–6. The agreement between the tracer and bulk values is excellent. The agreement can be taken to indicate that the approximation solution provides both a close and an adequate description of tracer events in the system from the point of view of conservation.

Steady-State Concentrations When Barriers Are Present At Capillary and Cell Surface

In most tissues substrates are delivered by flow through capillaries that have well-defined permeability properties, and metabolic removal processes take place in cells surrounded by interstitial tissue or extracellular space. In this kind of system there are two potential barriers to the distribution of substrates: one at the capillary and one at the parenchymal cell surface. When substrates are removed in this situation, concentration gradients will be expected to develop along the length of the capillary in the vascular space, the interstitial space, and the parenchymal cellular space.

In this case assume that the concentrations in space and time in capillary, interstitial, and cellular spaces are $u(x, t)$, $v(x, t)$, and $z(x, t)$ and that the space ratios γ and θ apply to interstitial and cellular spaces, as before. Then formulate the equations in a manner analogous to those developed by Rose et al. (25). The equation of conservation is

$$\frac{\partial u}{\partial t} + W\frac{\partial u}{\partial x} + \gamma\frac{\partial v}{\partial t} + \theta\frac{\partial z}{\partial t} + \frac{V_{max}\theta z}{(z + K_m)} = 0 \qquad (64)$$

The rate equation for accumulation in the interstitial space is

$$\frac{\partial v}{\partial t} = k_1 u - k_2 v - k_3 v + k_4 z \qquad (65)$$

and the rate equation for accumulation in the intracellular space is

$$\frac{\partial z}{\partial t} = \frac{\gamma}{\theta} k_3 v - \frac{\gamma}{\theta} k_4 z - \frac{V_{max} z}{(z + K_m)} \qquad (66)$$

These equations will apply only to well-perfused tissues. In tissues in which the distances between perfused capillaries are substantial in magnitude, times to diffusion equilibration in the radial direction will become substantial, and the effects of diffusion gradients in this direction would have to be introduced.

Now examine the steady-state response to a step input beginning at $t = 0$

$$u(0, t) = u_0 S(t)$$

TABLE 1. *Relative galactose outflow recoveries*

Galactose Concn, mM	$\tau = 2$ s		$\tau = 5$ s	
	Bulk	Tracer	Bulk	Tracer
0.1	0.422	0.422	0.115	0.111
0.5	0.506	0.508	0.151	0.151
2.0	0.765	0.767	0.444	0.440
10.0	0.946	0.944	0.866	0.865

The concentrations will then no longer be changing as a function of time. Hence *Eqs. 64-66* become

$$W\frac{du}{dx} + \frac{V_{max}\theta z}{z + K_m} = 0 \quad (67)$$

$$k_1 u - k_2 v - k_3 v + k_4 z = 0 \quad (68)$$

and

$$\frac{\gamma}{\theta} k_3 v - \frac{\gamma}{\theta} k_4 z - \frac{V_{max} z}{z + K_m} = 0 \quad (69)$$

Eliminating v from *Eqs. 68* and *69*, we find

$$\frac{k_1 k_3 \{\gamma/\theta\}}{(k_2 + k_3)} u = z\left[k_4\{\gamma/\theta\} - \frac{k_3 k_4 \{\gamma/\theta\}}{(k_2 + k_3)} + \frac{V_{max}}{z + K_m}\right] \quad (70)$$

Differentiating this with respect to x and eliminating du/dx from this equation and *Eq. 67*, we find

$$\left[\frac{R_1 K_m + V_{max}}{z} - \frac{V_{max}}{z + K_m} + R_1\right] dz = -R_2 \frac{dx}{W} \quad (71)$$

where $R_1 = k_4\{\gamma/\theta\} - k_3 k_4\{\gamma/\theta\}/(k_2 + k_3)$ and $R_2 = k_1 \gamma k_3 V_{max}/(k_2 + k_3)$, so that

$$\frac{z^{(R_1 K_m + V_{max})}}{(z + K_m)^{V_{max}}} e^{R_1 z} = \text{constant}\ e^{-R_2 \frac{x}{W}} \quad (72)$$

Now consider that, at $x = 0$, $u = u_o$ and $z = z_o$. Then, from *Eq. 70* we find that

$$R_1 z_o^2 + (R_1 K_m + V_{max} - R_3 u_o) z_o - R_3 K_m u_o = 0 \quad (73)$$

where

$$R_3 = k_1 k_3 \{\gamma/\theta\}/(k_2 + k_3).$$

Given u_o, the desired value for z_o will be the real and positive root of *Eq. 73*. Then, setting $x = 0$ in *Eq. 72*, we find that

$$\text{constant} = \frac{z_o^{(R_1 K_m + V_{max})}}{(z_o + K_m)^{V_{max}}} e^{R_1 z_o}$$

So that finally we have

$$\left[\frac{z_o + K_m}{z + K_m}\right]^{V_{max}} \left[\frac{z}{z_o}\right]^{R_1 K_m + V_{max}} e^{R_1 (z - z_o)} = e^{-R_2 \frac{x}{W}} \quad (74)$$

Given values for $z(x)$, concomitant values for $u(x)$ can be calculated from *Eq. 70* and values for $v(x)$ from *Eq. 68*. Expressions for all three adjacent space profiles have been developed.

Once again, consider the asymptotic extremes.

a) When z_o and $z \ll K_m$, then $z_o + K_m \rightarrow K_m$ and $z + K_m \rightarrow K_m$. We then find from *Eqs. 67-69* that

$$u = u_o e^{-\frac{k_1 \gamma k_3 (V_{max}/K_m)}{k_2 k_4 \{\gamma/\theta\} + k_2 \{V_{max}/K_m\} + k_3 \{V_{max}/K_m\}} \frac{x}{W}} \quad (75)$$

$$v = \frac{k_1 k_4 \{\gamma/\theta\} + k_1 (V_{max}/K_m)}{k_2 k_4 \{\gamma/\theta\} + k_2 \{V_{max}/K_m\} + k_3 \{V_{max}/K_m\}} z \quad (76)$$

and

$$z = \frac{k_1 k_3 \{\gamma/\theta\}}{k_2 k_4 \{\gamma/\theta\} + k_2 \{V_{max}/K_m\} + k_3 \{V_{max}/K_m\}} u \quad (77)$$

Each concentration decreases exponentially along the length, with the same space constant. There is a constant ratio between each compartment concentration at each point along the length. This linear asymptotic extreme corresponds to the set of steady-state profiles predicted by Rose et al. (25) in their exploration of linear uptake kinetics in the heart. The linear cellular removal rate constant is, in this case, V_{max}/K_m.

b) When z_o and $z \gg K_m$, we find from *Eqs. 67-69* that

$$u = (R_1 z + V_{max})/R_3 \quad (78)$$

$$v = (k_4/k_3) z + V_{max}/(\gamma/\theta) k_3 \quad (79)$$

$$z = z_o - R_2 (x/W) \quad (80)$$

The value for z_o can be calculated from that for u_o with *Eq. 78*. As expected the profiles have evolved from exponential at the low concentration extreme to slowly declining linear ones at the high concentration extreme.

The behavior of tracer within this steady state will be even more complex than when only one barrier exists in the system. In principle, it could be developed in a manner similar to that utilized for the one-barrier case. We have not carried out this exploration in the present paper; however, the approximate forms of the tracer equations for the cases when the concentration does not sweep across a large part of the range with respect to the K_m, in the single experiment, can be found quite simply by substituting the following expression for the uptake rate constant k_5 in the tracer *Eqs. 10-14* in the paper by Rose et al. (25)

$$k_5 = \frac{V_{max}}{(z + K_m)} \quad (81)$$

Discussion

Steady-state in vivo concentration profiles. The steady-state profiles predicted in the foregoing are firmly rooted in the idea that the metabolic removal step (either chemical transformation or secretion into the countercurrently transported canalicular bile) is evenly distributed in parenchymal cells along the length of the vascular channel. Profiles approaching the exponential have been found in no-load tracer experiments in the liver after the administration of labeled galactose (11) and of labeled cholylglycine (18), a bile acid derivative excreted in bile. Gumucio et al. (16) have explored the uptake of fluorescent compounds into hepatocytes and the zonal labeling of the hepatic acinus in the rat resulting from this uptake and have found space profiles for fluorescein diacetate, acridine orange, and rhodamine B that varied from exponential to essentially a flat linear profile, with increase in the dose of the material. Progressive recruitment of cells along the sinusoids was found to precede the attainment of saturation, as predicted in the present modeling.

Regionalization of enzymic processes could, of course, result in shapes of longitudinal space profiles differing from those predicted above. The local kinetic activity of the enzymic removal process will be proportional to the local enzyme concentration. Substrate concentration-space profiles will be expected to decrease more steeply in regions where the enzyme concentration is high and more gradually in regions where it is low. If the enzyme

were absent in the portal area and present in high concentration in the peripheral part of the acinus, near the terminal hepatic venules, the steady-state concentration would be uniform until it reached the region where the enzyme was situated and would then decrease in that area.

One also expects the discovery of additional physiological phenomena as local spatial concentration profiles are explored further. For instance, Gumucio et al. (16) found that, with increase in dose, the space profile for fluorescein isothiocyanate changes from one decreasing from input to exit to a reverse gradient, one increasing from input to exit. Comparison of the results with the modeling outlined above indicates that phenomena additional to those included in the modeling must be involved (the rising distal concentrations could reveal, for instance, a more highly concentrative membrane carrier transport process in the cells in the more distal part of the acinus; a larger concentration of an intracellular binding protein in this region; a regional pH value resulting in a larger proportion of the compound being in the fluorescent form; or a more brightly fluorescent product that is accumulating downstream). Comparison of observations with modeling results may thus provide a framework for the discovery of additional new processes.

When a process within the tissue simultaneously generates the substrate whose removal is being examined, the shapes of the predicted concentration profiles would also be expected to change. If such a process were regional, it would be expected to have a major influence on the space profiles.

Substrate space profiles will be expected to be developed best in studies in which the beginnings and endings of adjacent vascular channels are coterminal in space. The tissue exemplifying this architectural feature is the liver, and it is in this tissue that gradients have best been displayed on a microscopic scale. The search for similar gradients in other organs remains to be pursued.

Clearance measurements and pharmacokinetics. The central organ involved in the removal of many substances from the circulation is the liver. The description of the manner in which the liver extracts materials from the circulation thus is a central issue in pharmacokinetics. Previously, at the experimental level, conservation relations were used to describe uptake in an exceedingly simple fashion. For a protein-bound anionic dye in the steady state, its infusion rate was taken to be equal to the hepatic removal rate, and the removal rate was then set equal to the product of liver blood flow and the difference between input and output concentrations. Because portal venous and arterial concentrations were in general equal under this set of circumstances, it was then only necessary to obtain arterial and hepatic venous blood samples to determine liver blood flow. To characterize the removal process more closely, it is necessary to characterize net organ extractions over a wide range of concentrations and to knit the observations into a recognizable whole.

The first part of the present development, in which there are no effective barriers in the liver for the substance being removed, has been examined from this point of view (29). Remembering that $\nu = F_w(u_o - u_L)$ and defining clearance as $F_w(u_o - u_L)/u_o$, then for the whole liver the clearance $\nu/u_o = \Sigma F_w(u_o - u_L)/u_o$, where there is a heterogeneity of flows and outflow concentrations across the population of liver sinusoids (13). This heterogeneity of flows and outflow concentrations has initially been treated simply by assuming that some average set of values can be found that are representative of the whole and that these can be used in the equation describing bulk uptake along the single sinusoid. Winkler et al. (29), for instance, have shown, by integrating *Eq. 8* in a straightforward fashion, that for this representative single sinusoid

$$u_L = u_o e^{-\left(\frac{V_{tc}-\nu}{F_w K_m}\right)}$$

so that

$$\nu/u_o = F_w\left[1 - e^{-\left(\frac{V_{tc}-\nu}{F_w K_m}\right)}\right] \tag{82}$$

This expression for clearance is, in a sense, a solution alternate to that given in *Eq. 9*. In this instance, V_{tc} represents the maximal rate of substrate removal by the organ (in the units amount·time^{-1}); it is the product of V_{max}, the rate of removal per unit cellular volume [with the units amount·(ml liver cells)$^{-1}$·time^{-1}] and the total volume of parenchymal cells in the liver in milliliters.

The asymptotic forms are again of interest.

a) When u_o and $u_L \ll K_m$, $\nu \ll V_{tc}$ and

$$\nu/u_o \to F_w\left[1 - e^{-\left(\frac{V_{tc}}{F_w K_m}\right)}\right] \tag{83}$$

This is the linear lower concentration extreme, in which extraction is independent of the value of u_o. Because, in this extreme, the extraction is dependent on the ratio V_{tc}/K_m and is otherwise dependent only on flow, this extreme has been called the "systemic clearance" regime. It represents the extreme most easily integrated with ordinary pharmacokinetic modeling.

In the development in this paper we have shown that these equations describe uptake of a material delivered to the enzymic mechanism within cells in a flow-limited fashion. The magnitude of the ratio V_{tc}/K_m will dictate the proportion of the material extracted during passage through the liver at this lower concentration extreme. If this ratio is large, the net extraction will be large; if it is small, the net extraction will be small. Winkler et al. (29) have mistakenly considered these two ends of the low-concentration extreme to be "flow limited" and "enzyme limited." The development we outlined in the present paper indicates that the equations developed for this low concentration extreme describe a case that is always flow limited and that the proportional extraction in this flow-limited case depends directly on the ratio V_{tc}/K_m.

b) When u_o and $u_L \gg K_m$, $\nu \to V_{tc}$, and $V_{tc} - \nu$ becomes very small. In this limit e^{-a} can be considered adequately represented by the first two terms of the Taylor expansion, $1 - a$. Then

$$\nu/u_o \to F_w[1 - (1 - \{V_{tc} - \nu\}/F_w K_m)]$$

or

$$\nu/u_o \to (V_{tc} - \nu)/K_m$$

There is no particularly useful information in this equation. The clearance progressively decreases towards zero as ν increases. What is important is that, in this extreme, $\nu \rightarrow V_{tc}$ and that, experimentally, V_{tc} is thus accessible to measurement.

Two further matters bear discussion in this simplest case, in which there are no effective barriers in the system: *1*) in the area of pharmacokinetics it has been suggested that hepatic outflow concentrations can be used as an approximation of the sinusoidal concentration (6); and *2*) ν/u_L, the "intrinsic clearance," in which the rate of removal is related to the outflow concentration, is a flow-independent measure of some importance (28). By definition, the measure is not flow independent, and our theoretical analysis of the uptake kinetics in this situation, as well as that of Bass et al. (1), indicates that the concentration that it is necessary to consider if one is to obtain appropriate estimates of the V_{tc} and K_m parameters is neither the input nor the outflow concentration but rather $\hat{u}$, the logarithmic average concentration. The second matter relates to utility of the flow-limited case in more general pharmacokinetic modeling schemes. In this simplest case, with no barrier in the system across which concentration inequalities will build up, the scheme developed to describe steady-state bulk removal can be incorporated into more general pharmacokinetic schemes, in which bulk concentrations are allowed to sweep across a wide range.

The present development also indicates that none of the foregoing can be applied to analysis of the situation in which the cell membrane acts as a functional barrier. The existence of the barrier will allow concentration inequalities to build up across membrane (5, 11) and will introduce a whole new set of transient phenomena across the membrane (parallel lengthwise concentration gradients will evolve continually as a result of changing saturation of the removal mechanism as the removal proceeds). At present, there is no adequate analytical description of this set of phenomena that would be useful for the analysis of bulk intravenous disappearance curves, where bulk concentrations are changing with time. Forker and Luxon (5) have provided a qualitative assessment of events expected under this set of conditions by numerically inverting the appropriate Laplace transforms after convolution of the liver model with a model of events at the level of both the central circulation and the rest of the body. The way to then utilize this in the analysis of intravenous disappearance curves remains to be defined.

We thank Dr. John Jacquez, who by his interactions during the review process enabled us to find an appropriate approach to the tracer saturation problem, and Dr. Ken Zierler for his stimulating discussion. We also express our appreciation to Kim McMillan, Louise Gagnon, and Laurie-Ellen Gwynne for their technical assistance; to Margaret Mulherin and Pamela Lilley for typing the manuscript; and to the Medical Research Council of Canada, the Quebec Heart Foundation, the Edwards Foundation, and the Department of Medicine of the Montreal General Hospital for their financial support.

C. A. Goresky is the recipient of a Career Investigator Award and C. P. Rose, a Scholarship from the Medical Research Council of Canada.

Address for reprint requests: C. A. Goresky, University Medical Clinic, Montreal General Hospital, 1650 Cedar Ave., Montreal, Quebec H3G 1A4, Canada.

Received 11 December 1980; accepted in final form 13 August 1982.

REFERENCES

1. Bass, L., S. Keiding, K. Winkler, and N. Tygstrup. Enzymatic elimination of substrates flowing through the intact liver. *J. Theor. Biol.* 61: 393–409, 1976.
2. Bassingthwaighte, J. B. A concurrent flow model for extraction during transcapillary passage. *Circ. Res.* 35: 483–503, 1974.
3. Bassingthwaighte, J. B., T. J. Knopp, and J. B. Hazelrig. A concurrent flow model for capillary-tissue exchange. In: *Capillary Permeability*, edited by C. Crone and N. A. Lassen. Copenhagen, Denmark: Munksgaard, 1970, p. 60–80.
4. Fersht, A. *Enzyme Structure and Mechanism*. San Francisco, CA: Freeman, 1979.
5. Forker, E. L., and B. Luxon. Hepatic transport kinetics and plasma disappearance curves: distributed modeling versus the conventional approach. *Am. J. Physiol.* 235 (*Endocrinol. Metab. Gastrointest. Physiol.* 4): E648–E660, 1978.
6. Gillette, J. R., Factors affecting drug metabolism. *Ann. NY Acad. Sci.* 174: 43–66, 1971.
7. Gonzalez-Fernandez, J. M., and S. E. Atta. Maximal substrate transport in capillary networks. *Microvasc. Res.* 5: 180–198, 1973.
8. Goresky, C. A. A linear method for determining liver sinusoidal and extravascular volumes. *Am. J. Physiol.* 204: 626–640, 1963.
9. Goresky, C. A. Initial distribution and rate of uptake of sulfobromophthalein by the liver. *Am. J. Physiol.* 207: 13–26, 1964.
10. Goresky, C. A., G. G. Bach, and B. E. Nadeau. On the uptake of materials by the intact liver: the concentrative uptake of rubidium-86. *J. Clin. Invest.* 52: 975–990, 1973.
11. Goresky, C. A., G. G. Bach, and B. E. Nadeau. On the uptake of materials by the intact liver: the transport and net removal of galactose. *J. Clin. Invest.* 52: 991–1009, 1973.
12. Goresky, C. A., G. G. Bach, and B. E. Nadeau. Red cell carriage of label: its limiting effect on the exchange of materials in the liver. *Circ. Res.* 36: 328–351, 1975.
13. Goresky, C. A., E. R. Gordon, and G. G. Bach. Uptake of monohydric alcohols by liver: demonstration of a shared enzymic space. *Am. J. Physiol.* 244 (*Gastrointest. Liver Physiol.* 7): G198–G214, 1983.
14. Goresky, C. A., and B. E. Nadeau. Uptake of materials by the intact liver: the exchange of glucose across the cell membranes. *J. Clin. Invest.* 53: 636–646, 1974.
15. Goresky, C. A., and C. P. Rose. Blood-tissue exchange in liver and heart: the influence of the heterogeneity of capillary transit times. *Federation Proc.* 36: 2629–2634, 1977.
16. Gumucio, J. J., D. L. Miller, M. D. Krauss, and C. C. Zanalli. The transport of fluorescent compounds into hepatocytes and the resultant zonal labeling of the hepatic acinus in the rat. *Gastroenterology* 80: 639–646, 1981.
17. Henry, V. *Lois Générale de L'Action des Diastases*. Paris: Hermann, 1901.
18. Jones, A. L., G. T. Hradek, R. H. Renson, K. Y. Wong, G. Karlaganis, and G. Paumgartner. Autoradiographic evidence for hepatic lobular concentration gradient of bile acid derivative. *Am. J. Physiol.* 238 (*Gastrointest. Liver Physiol.* 1): G233–G237, 1980.
19. Keiding, S., S. Johansen, I. Midtbøll, A. Rabøl, and L. Christiansen. Ethanol elimination kinetics in human liver and pig liver in vivo. *Am. J. Physiol.* 237 (*Endocrinol. Metab. Gastrointest. Physiol.* 6): E316–E324, 1979.
20. Keiding, S., S. Johansen, K. Winkler, K. Tonneson, and N. Tygstrup. Michaelis-Menten kinetics of galactose elimination by the isolated perfused pig liver. *Am. J. Physiol.* 230: 1302–1313, 1976.
21. Michaelis, L., and M. L. Menten. Die Kinetik der Invertinwirkung. *Biochem. Z.* 49: 333–369, 1913.
22. Ralston, A. *A First Course in Numerical Analysis*. New York: McGraw, 1965, p. 323–328.
23. Rappaport, A. M. Hepatic blood flow: morphological aspects and physiologic regulation. In: *Liver and Biliary Tract Physiology*, edited by N. B. Javitt. Baltimore, MD: Univ. Park Press, 1980, p. 1–63.

24. ROSE, C. P., AND C. A. GORESKY. Vasomotor control of capillary transit time heterogeneity in the canine coronary circulation. *Circ. Res.* 39: 541–554, 1976.
25. ROSE, C. P., C. A. GORESKY, AND G. G. BACH. The capillary and sarcolemmal barriers in the heart: an exploration of labeled water permeability. *Circ. Res.* 41: 515–533, 1977.
26. TYGSTRUP, N., AND K. WINKLER. Kinetics of galactose elimination. *Acta Physiol. Scand.* 32: 354–362, 1954.
27. WHEELER, H. O., J. I. MELTZER, AND S. E. BRADLEY. Biliary transport and hepatic storage of sulfobromophthalein in the unanesthetized dog, in normal man, and in patients with hepatic disease. *J. Clin. Invest.* 39: 1131–1144, 1960.
28. WILKINSON, G. R., AND D. G. SHAND. A physiological approach to hepatic drug clearance. *Clin. Pharmacol. Ther.* 18: 377–390, 1975.
29. WINKLER, K., L. BASS, S. KIEDING, AND N. TYGSTRUP. The physiological basis for clearance measurements in hepatology. *Scand. J. Gastroenterol.* 14: 439–448, 1979.